

Experimental Genuine Tripartite Nonlocality in a Quantum Triangle Network

Alessia Suprano¹,¹ Davide Poderini,^{1,2} Emanuele Polino,¹ Iris Agresti,¹ Gonzalo Carvacho¹,¹ Askery Canabarro^{2,3},^{2,3} Elie Wolfe⁴,⁴ Rafael Chaves,^{2,5} and Fabio Sciarrino^{1,*}

¹*Dipartimento di Fisica—Sapienza Università di Roma, P. le Aldo Moro 5, Roma I-00185, Italy*

²*International Institute of Physics, Federal University of Rio Grande do Norte, Natal, Região Nordeste 59078-970, Brazil*

³*Grupo de Física da Matéria Condensada, Núcleo de Ciências Exatas—NCEX, Campus Arapiraca, Universidade Federal de Alagoas, Arapiraca, Alagoas 57309-005, Brazil*

⁴*Perimeter Institute for Theoretical Physics, 31 Caroline St. N, Waterloo, Ontario, N2L 2Y5, Canada*

⁵*School of Science and Technology, Federal University of Rio Grande do Norte, Natal, Região Nordeste 59078-970, Brazil*



(Received 14 April 2022; accepted 16 August 2022; published 21 September 2022)

Quantum networks are the center of many of the recent advances in quantum science, not only leading to the discovery of new properties in the foundations of quantum theory but also allowing for novel communication and cryptography protocols. It is known that networks beyond that in the paradigmatic Bell's theorem imply new and sometimes stronger forms of nonclassicality. Due to a number of practical difficulties, however, the experimental implementation of such networks remains far less explored. Going beyond what has been previously tested, here we verify the nonlocality of an experimental triangle network, consisting of three independent sources of bipartite entangled photon states interconnecting three distant parties. By performing separable measurements only and evaluating parallel chained Bell inequalities, we show that such networks can lead to a genuine form of tripartite nonlocality, where classical models are unable to mimic the quantum predictions even if some of the parties are allowed to communicate.

DOI: [10.1103/PRXQuantum.3.030342](https://doi.org/10.1103/PRXQuantum.3.030342)

I. INTRODUCTION

Bell nonlocality [1–3] offers a vast research landscape with relevance for foundational [4–7] and quantum technological applications ranging from secure quantum communication protocols [8–13] and randomness generation and certification [14–18] to self-testing of quantum devices [19] and distributed computing [20,21].

Moving beyond the paradigmatic Bell scenario, the causal perspective on nonclassicality [22–24] has illuminated the fact that new and sometimes stronger forms of nonlocality can arise [24–53]. A particularly relevant situation is that of a network involving several parties and independent sources, a scenario akin to what one can expect from the first small to midsized quantum networks under development [12] aiming at a future large-scale quantum

Internet [54,55]. In such networks, instead of having all distant nodes connected by a single source (as would be the case in Bell's theorem), producing a fragile many-qubit state, the correlations are mediated by many sources generating states of small size and thus enhanced robustness and quality, e.g., bipartite entangled states.

In spite of significant theoretical progress, understanding the correlations that such quantum networks can give rise to (see, e.g., the recent review in Ref. [56]), the experimental side of this effort [57–65] is far less unexplored, due to a number of practical difficulties. In the particular case of a photonic platform, the most prominent of these difficulties stems from the probabilistic nature of the generation of the photons and the synchronization process, which becomes exponentially more demanding as the number of entanglement sources increase. Furthermore, in many cases there is a need for entangled measurements, a requirement that can only be partially achieved with linear optics or that requires device-dependent assumptions for the experimental implementation [57,58]. These issues are worsened when the independence of the sources is required to be physically justified, e.g., by using different and non-synchronized lasers to pump the generation crystals that act

*fabio.sciarrino@uniroma1.it

Published by the American Physical Society under the terms of the [Creative Commons Attribution 4.0 International](https://creativecommons.org/licenses/by/4.0/) license. Further distribution of this work must maintain attribution to the author(s) and the published article's title, journal citation, and DOI.

as sources [64]. For this reason, only two examples of photonic networks involving independent sources have been implemented in a device-independent manner so far [66], one concerning the bilocality scenario [57–59,63,65] and the other a star network with four sources [64].

Genuine multipartite nonlocality plays an important role in the context of multipartite networks. This concept was originally introduced by Svetlichny [67] with the intention of distinguishing those correlations the nonclassicality of which does not reduce to merely bipartite nonclassicality. For Svetlichny, this distinction could only be attained by witnessing the violation of a Bell-like inequality bounding those classical models where all but one of the parties might communicate among themselves. Note that multiple variants of his definition have been introduced in more recent literature [68,69] to ensure consistency with resource theories allowing for bipartite processing of nonlocal boxes.

Perhaps counterintuitively, Svetlichny’s notion of nonlocality does *not* require multipartite quantum sources to be manifest; rather, such correlations can be realized in a network consisting of only bipartite sources [70–72]. Unfortunately, existing proofs of this fact rely on *pure* bipartite entangled states and hence are unsuitable for experimental demonstration. In this work, we provide new *robust* proofs of this fact by showing how the cumulative payoff of multiple bipartite nonlocal games played in parallel can effectively witness Svetlichny’s genuine multipartite nonlocality. Not only do such parallel-payoff inequalities have the advantage of being analytically derivable but they are also violable under feasible experimental conditions. To prove this, we analyze the robustness of such parallel inequalities, thereby contrasting various multipartiteness witnesses for general network scenarios. This initial analysis lets us identify the most suitable configuration of parallel-bipartite nonlocal games for experimentally verifying such multipartiteness. The optimal corresponding network structure is found to be the *quantum triangle*, notably a structure of extensive recent interest [24–39].

The triangle scenario is composed of three independent two-way sources distributing entanglement out to three parties, such that each source is shared between only two parties and such that each party receives systems from only two sources.

Differently from the typical analysis in the literature [24–29], here we consider the situation where each of the three parties can perform a number of separable and independent measurements on each of the qubits in their possession. We experimentally realize the quantum triangle network using a platform based on the scheme of Ref. [64], showing that we can achieve genuine tripartite nonlocality without the (demanding) employment of tripartite sources [73,74].

The paper is organized as follows. Section II introduces both Bell’s theorem [1] and Svetlichny’s notion

of genuine multipartite nonlocality [67] from a causal perspective, highlighting how the latter can be achieved merely by playing bipartite nonlocal games in parallel. In Sec. III, we present a robustness analysis of parallel nonlocal games in general bipartite networks, thereby obtaining criteria for identifying optimal scenarios and inequalities for experimental demonstration. In Sec. IV, we describe our experimental implementation of the quantum triangle network, and discuss the extent to which our observed statistics witness genuine multipartiteness.

II. BELL’S THEOREM AND CAUSAL STRUCTURES

Bell’s theorem [1] is typically cast as the incompatibility of quantum predictions with those expected from theories respecting local causality, the latter formally expressed by local-hidden-variable (LHV) models. More specifically, two distant parties, Alice and Bob, receive their shares of a physical system produced by a source that classically is represented by a random variable λ . Since we cannot assume that we have access to all relevant degrees of freedom of the source, λ is treated as a hidden variable, information about which we can only gather via measurements. Upon receiving their part of the joint physical system, the parties randomly decide which kind of measurement to perform, a choice parametrized by the variables x_1 and x_2 with corresponding outcomes a_1 and a_2 for Alice and Bob, respectively. Any observable probability distribution $p(a_1, a_2|x_1, x_2)$ compatible with the LHV assumptions can then be decomposed as

$$p(a_1, a_2|x_1, x_2) = \sum_{\lambda} p(a_1|x_1, \lambda)p(a_2|x_2, \lambda)p(\lambda), \quad (1)$$

where we explicitly employ the causal assumptions in Bell’s theorem. First, the locality assumption states that the outcome of Alice (and similarly for Bob) should only depend on the variables on her causal past (thus the necessity of spacelike separation between Alice and Bob). It implies that $p(a_1|x_1, x_2, a_2, \lambda) = p(a_1|x_1, \lambda)$ (and similarly for Bob). In turn, the measurement-independence assumption (also known as free will) states that $p(x_1, x_2, \lambda) = p(x_1, x_2)p(\lambda)$ and encompasses the basic idea that the observers should have the freedom to choose which observable to measure independently of how the system under measurement is prepared. Implicit is the realism assumption, represented by the fact that the LHV model assumes the existence of the variable λ subsuming well-defined probabilities for all possible outcomes, even for those measurements that are not performed.

From a more modern perspective, we can see Bell’s theorem as the fact that a classical causal model cannot reproduce the quantum correlations, that according to

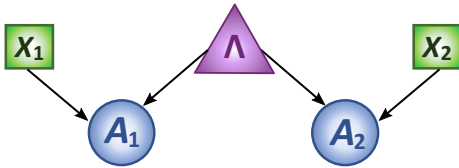


FIG. 1. The directed-acyclic-graph (DAG) representation of the bipartite Bell scenario. A classical source described by the random variable Λ underlies the correlations observed between the measurement outcomes of two distant parties.

Born's rule are given by

$$p(a_1, a_2 | x_1, x_2) = \text{Tr} \left[(M_{a_1}^{x_1} \otimes M_{a_2}^{x_2}) \rho \right], \quad (2)$$

where $M_{a_1}^{x_1}$ are positive operator-valued measure (POVM) operators describing Alice's measurements (and similarly for Bob) and ρ is the density operator representing the physical system shared between Alice and Bob. We are imposing a given causal structure to the experiment, that classically is represented via a directed acyclic graph (DAG) in Fig. 1. From the causal Markov condition [75]—implying that a given node of the graph should be independent of all its nondescendants given its parents—we obtain exactly the LHV decomposition given in Eq. (1). That is, in order to explain quantum correlations, we have to consider a quantum version of a causal model [30,31,33,76].

A straightforward generalization of Bell's theorem is to consider the multipartite scenario where all n distant parties are connected by a single source [2]. Classically, the observed correlation should thus be decomposable as

$$p(a_1, \dots, a_n | x_1, \dots, x_n) = \sum_{\lambda} p(a_1 | x_1, \lambda) \cdots p(a_n | x_n, \lambda) p(\lambda).$$

Just as in the bipartite case, allowing for the source to be quantum can give rise to distributions strictly outside the set of multipartite LHV distributions. This may seem trivial at first: if quantum violation can be achieved in the bipartite scenario, surely quantum violation can be achieved in the multipartite scenario. One needs only to consider *bipartite marginals* of a tripartite scenario to observe quantum advantage. What makes the multipartite scenario interesting, then, is that the sorts of operational advantages afforded by a tripartite quantum source are qualitatively distinct from the more limited advantages afforded by bipartite quantum sources. Early pioneers of the study of multipartite nonlocality were therefore motivated to define a notion of *genuine multipartiteness* of a nonclassical correlation. The original definition for genuine multipartiteness was proffered by Svetlichny in 1987 [67]. As with all subsequent definitions of genuine multipartiteness, Svetlichny's definition is apophatic, that is, a

distribution obtained by quantum strategies is said to be genuinely multipartite if it *cannot* be explained by a suitable foil theory. The foil theory that Svetlichny envisions is entirely classical but it is a theory wherein all but one of the involved parties can communicate with each other [49,50,67] and wherein the strict subset of parties that may communicate need not be fixed but can depend on a hidden variable.

For instance, in the tripartite scenario, we can consider a convex combination of models, where any two of the parties can communicate arbitrarily among them, a situation that can, without loss of generality [50], be described by the communication of inputs between the parties, with the corresponding DAG shown in Fig. 2(a) for the case where parties 1 and 2 are the communicating ones. The classical description of the tripartite probability distribution is thus given by

$$p(a_1, a_2, a_3 | x_1, x_2, x_3) = q_1 p_{a_1 \leftrightarrow a_2} + q_2 p_{a_1 \leftrightarrow a_3} + q_3 p_{a_2 \leftrightarrow a_3},$$

where $q_1 + q_2 + q_3 = 1$, and

$$p_{a_1 \leftrightarrow a_2} = \sum_{\lambda} p(a_1 | x_1, x_2, \lambda) p(a_2 | x_1, x_2, \lambda) \times p(a_3 | x_3, \lambda) \quad (3)$$

is the nonlocal classical model represented by the DAG in Fig. 2(a) (and similarly for the terms $p_{a_1 \leftrightarrow a_3}$ and

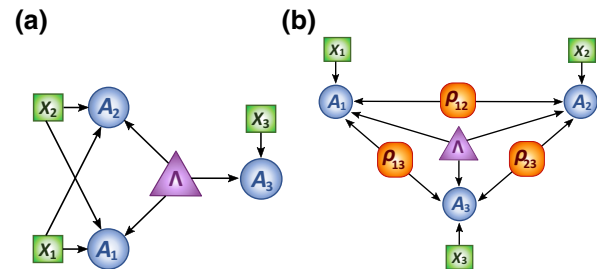


FIG. 2. DAG representations of tripartite networks. (a) In the tripartite Svetlichny scenario—i.e., in the causal structure of Svetlichny's classical foil theory—a classical source described by the random variable Λ underlies the correlations observed between the measurement outcomes of the three parties. In contrast to Bell's local-hidden-variable (LHV) models per Fig. 1, however, in Svetlichny's scenario any two of the parties can communicate, without loss of generality, by exchanging their inputs. Which pair of parties are in communication may also depend on Λ , though this additional freedom is not explicitly depicted here. (b) A conceptual scheme of the apparatus realizing a quantum triangle network. Note the three independent quantum sources ρ_{12} , ρ_{13} , and ρ_{23} that are shared between the different pairings of the three parties. In practice, the classical common cause Λ is only used to establish a common reference frame. Our main result is that by allowing the noncentral sources in (b) to be quantum, we can experimentally achieve correlations that cannot be explained in (a).

$p_{a_2 \leftrightarrow a_3}$). Hereafter, we abbreviate the oft-referred to concept of Svetlichnyesque genuine multipartite nonlocality as *SGMNL*.

To achieve SGMNL correlations, we would require entanglement *beyond* the sort achievable from scratch with local operations and classical communication (LOCC) and a quantum channel connecting only two of the three parties in the network. For this reason, Svetlichny's definition for genuine multipartite nonlocality serves as a device-independent witness of genuine multipartite entanglement.

Intuitively, one might think that Svetlichny's definition is meant to distinguish certain correlations realized by a three-way quantum source from those that can be realized from two-way quantum sources, but this is incorrect. SGMNL is tailored to witness *nonrealizability by LOCC and quantum channels only between a strict subset of the parties*. As such, Svetlichny's definition can be *hacked*: using only local operations on bipartite quantum sources—without even making use of shared randomness or even classical communication between strict subsets of parties—one can realize SGMNL correlations. The causal structure of this so-called “triangle” scenario is depicted in Fig. 2(b), such that a *quantum* distribution that can be realized in such a scenario is of the form

$$p^Q(a_1, a_2, a_3 | x_1, x_2, x_3) = \text{Tr}(\rho_{12} \otimes \rho_{13} \otimes \rho_{23} M_{x_1}^{a_1} \otimes M_{x_2}^{a_2} \otimes M_{x_3}^{a_3}) \quad (4)$$

where ρ_{ij} represents the bipartite quantum state generated by the source Λ_{ij} and $M_{x_i}^{a_i}$ are the opportunely ordered POVMs associated with node i , such that $\sum_{a_i} M_{x_i}^{a_i} = \mathbb{1}$, for all x_i .

The main result of this paper is an experimental demonstration of the achievement of SGMNL using a quantum triangle causal structure. In fact, we further tie our hands behind our backs and showcase Svetlichnyesque multipartiteness from *product* measurements on bipartite sources. At this point, it is worth remarking on an issue present in most experimental implementations of quantum networks but that nevertheless has no impact in our experiment. While in a usual Bell test resorting to a single source of correlations, shared reference frames (necessary to, e.g., calibrate measurement-apparatus setups between distant stations) do not change the causal structure under test, this is no longer true for networks involving independent sources. As detailed in Ref. [59], the use of shared reference frames can be seen as a common hidden variable between all measurement outcomes, which would break the assumption that the correlations are established solely by independent sources. Nevertheless, in our experiment, the presence of a shared reference frame between all distant measurement stations is not an issue. We are testing quantum correlations against the classical Svetlichny model in Fig. 2(a), which not only allows for communication between some of the parts but also for the presence of such global hidden

variables, this being the reason why we explicitly include it in the DAG description of our triangle experiment in Fig. 2(b).

Although multiple prior works have recognized the susceptibility in Svetlichny's definition discussed above, all prior proofs are remarkably unsuitable for experimental implementation. Accordingly, we briefly review some relevant theory results, but then we derive novel inequalities for witnessing SGMNL that are amenable to experimental analysis.

In Refs. [73,77], it is shown that local wirings [78] of extremal bipartite nonsignaling boxes lead to SGMNL. Local wirings are a form of local operations and this does constitute a triangle-scenario causal structure achieving SGMNL but the protocols in Refs. [73,77] rely on postquantum resources and hence their ideas cannot be adapted for quantum experimentation. In Ref. [70], it is proved that entanglement swapping can asymptotically lead to steering to a maximally entangled pair of qubits on any hub-and-spoke node pair in the star network, which implies SGMNL per the results of Ref. [71]. Our goal is to use product measurements, however, and in any case, asymptotics are not amenable to experimentation. Nevertheless, in Refs. [70,71] it is proved that SGMNL can arise in principle from local operations of parties in a network defined by merely bipartite quantum states. In Ref. [72], it is taken this one step further and the authors show that any star network composed of bipartite entangled pure states admits local measurements that give rise to SGMNL correlations. From an experimental perspective, the proof in Ref. [72] that SGMNL can be achieved without *maximal* entanglement is appreciated but since that proof continues to rely on *pure* states and *noiseless* measurements, it too is not amenable to experimental investigation.

Our perspective is to consider *parallel nonlocal games* such as they might be implemented in the triangle-like scenario of Fig. 3(b) or in more general scenarios. In general, we can model such a network as a graph, with nodes corresponding to parties and edges corresponding to a pair of parties playing an instance of a nonlocal game. We can then ask about the *maximum total payoff* of all parallel nonlocal games if the correlations are limited to those explainable by Svetlichny's foil theory. For instance, the classical tripartite correlations that can be explained by the DAG in Fig. 2(a) are such that, for three nonlocal games being played in parallel in the triangle scenario, the total score would have to satisfy

$$I^{12} + I^{13} + I^{23} \leq 2B_L + B_S, \quad (5)$$

where I_{ij} is a generic bipartite Bell inequality between parties i and j , given by

$$I_{ij} = \sum \alpha_{a_{ij}, a_{ji}, x_i, x_j} p(a_{ij}, a_{ji} | x_i, x_j) \leq B_L, \quad (6)$$

in which a_{ij} is the measurement outcome related to the measurement performed by party i on its state shared with party j . A given outcome a_i in the triangle can be understood as the composition of such individual outcomes, e.g., $a_1 = (a_{12}, a_{13})$. Continuing, B_L is the local bound achievable by LHV models of the form given in Eq. (1) and B_S is the algebraic maximum that can be obtained by a non-local-hidden-variable (NLHV) model where both parties can communicate with each other. The proof of this inequality follows from the analysis in Ref. [50] and can be intuitively understood as follows. If the parties 1 and 2 can communicate, then they can achieve the bound B_S ; however, since the parties 1 and 3 as well as 2 and 3 cannot communicate, they are indeed limited by the local bound B_L . In particular, note that the same argument holds for

any permutation of which two parties can communicate, thus leading to the Bell inequality given in Eq. (5), which bounds Svetlichny’s model in Eq. (3).

III. OPTIMIZATION OF A QUANTUM EXPERIMENT

Let a graph define a sum of bipartite Bell inequalities in the manner described above. That is, the triangle graph [Fig. 3(b)] corresponds to $I^{12} + I^{13} + I^{23}$, the tripartite-line graph [Fig. 3(a)] to $I^{12} + I^{23}$, and the divided-square graph [Fig. 3(c)] to $I^{12} + I^{13} + I^{23} + I^{14} + I^{34}$.

Lemma 1 (Total Payoff within Svetlichny’s Foil Theory). *The total score associated with a given graph G over correlations that are not SGMNL [79] is upper bounded by*

$$\max_{v \in \text{vertices}_G} \left(\begin{array}{l} B_S \times [\text{number of edges not connected to } v] \\ + B_L \times [\text{number of edges connected to } v] \end{array} \right) = B_S \times [\text{number of edges of } G] - (B_S - B_L) \min_{v \in \text{vertices}_G} [\text{number of edges connected to } v].$$

On the other hand, the total score under quantum strategies is just the quantum bound times the number of edges.

Lemma 2 (Total Payoff with Bipartite Quantum Strategies). *The total score associated with a given graph G over correlations achieved by playing quantumly realizable*

bipartite nonlocal games in parallel is

$$B_Q \times [\text{number of edges of } G],$$

or, for imperfect realizations,

$$(v B_Q + (1 - v) B_N) \times [\text{number of edges of } G],$$

where B_N is the payoff score of the nonlocal game under white noise. For all the Bell inequalities that we consider, we have $B_N = 0$, which makes the noise threshold for quantum achievement of SGMNL quite straightforward.

Corollary 3 (Visibility for SGMNL via Bipartite Quantum Strategies). *If an experiment can achieve quantum correlations with visibility v and $B_N = 0$, then playing such a correlation in parallel according to graph G yields SGMNL whenever*

$$v > \frac{B_S}{B_Q} - \frac{(B_S - B_L) \min_{v \in \text{vertices}_G} [\text{number of edges connected to } v]}{B_Q \times [\text{number of edges of } G]}.$$

Thus, to achieve SGMNL using parallel-bipartite strategies, one should optimize the *particular Bell inequality* (bipartite nonlocal game) corresponding to every edge in the graph and one should also optimize the *graph itself* to ensure that the ratio of B_S -scoring games to B_L -scoring games is as small as possible.

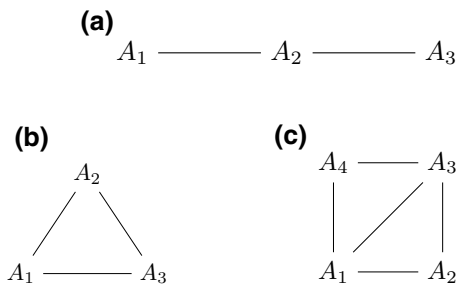


FIG. 3. A graph representation of nonlocal games. We can represent a particular configuration of a nonlocal game, composed by parallel-bipartite ones, using an undirected graph, where each node represents a party and two nodes are connected by an edge if the corresponding bipartite game appears in the payoff function. The figure shows two instances of possible configurations for tripartite games; the tripartite line (a) consisting of two parallel-bipartite games and the triangle (b) consisting of three parallel-bipartite games. We also depict a quadripartite (divided-square) scenario (c) consisting of five parallel-bipartite games.

A. Optimization of the Bell inequality

Before invoking multisetting generalizations, let us consider the Clauser-Horne-Shimony-Holt (CHSH) inequality. This inequality notably has $B_S = 4$, $B_L = 2$, $B_Q = 2\sqrt{2}$, and $B_N = 0$. Does this lead to SGMNL? In some graphs, yes; in other graphs, no. For instance, in the tripartite-line graph, the required v per Corollary 3 for CHSH would exceed unity; in other words, parallel CHSH with quantumly realizable scores *cannot* be used to witness SGMNL in the tripartite-line scenario.

At first, one might think that this could be an artifact of the Corollary 3 being a *sufficient but not necessary* criterion for witnessing SGMNL. However, we can *explicitly*

reconstruct the correlations associated with parallel quantum CHSH in the tripartite-line graph via a convex mixture of the extremal correlations realizable in Fig. 2(a) (and relabeling thereof). To see this, let P_{PR}^{ij} denote a Popescu-Rohrlich (PR) box between parties i and j , which yields a CHSH score of $+4$. Let P_{PR}^{ij} denote the anti-PR box between parties i and j , which yields a CHSH score of -4 . Let $P_{\text{mix}}^{ij}(v) := v \times P_{\text{PR}}^{ij} + (1 - v) \times P_{\text{PR}}^{ij}$. In this notation, the Tsirelson box [80], which gives $\text{CHSH} = 2\sqrt{2}$, is given by $P_{\text{Tsirelson}}^{ij} = P_{\text{mix}}^{ij} \left(\left(2 + \sqrt{2}\right) / 4 \right)$. The reader may verify that

$$P_{\text{Tsirelson}}^{12} \otimes P_{\text{Tsirelson}}^{23} = \left(w \frac{P_{\text{mix}}^{12}(1) \otimes P_{\text{mix}}^{23}(3/4) + P_{\text{mix}}^{12}(3/4) \otimes P_{\text{mix}}^{23}(1)}{2} + (1 - w) \frac{P_{\text{mix}}^{12}(0) \otimes P_{\text{mix}}^{23}(1/4) + P_{\text{mix}}^{12}(1/4) \otimes P_{\text{mix}}^{23}(0)}{2} \right), \quad (7)$$

where $w = (3 + 2\sqrt{2})/6 \approx 0.971$. This provides an explicit convex decomposition of parallel Tsirelson boxes in terms of four boxes that are themselves clearly members of the Svetlichny polytopes (i.e., the sets of correlations achievable with classical communication between two of the three parties) [81].

On the other hand, the CHSH inequality *does* lead to SGMNL for the *triangle* graph [Fig. 3(b)], as Corollary 3 tells us that playing CHSH in parallel per the triangle graph witnesses SGMNL down to a visibility of $v \approx 0.943$.

Note that this clarifies the potentially misleading statement in Ref. [82], which states that “the correlations obtained from CHSH violations in parallel between Alice and Bob as well as between Bob and Charlie fulfill Svetlichny’s criterion for genuine tripartite nonlocality.” That is true algebraically, as parallel *PR* boxes in the tripartite-line scenario [Fig. 3(a)] are SGMNL, but parallel *Tsirelson* boxes are *not* SGMNL in the tripartite-line scenario, though they are SGMNL in the triangle scenario [Fig. 3(b)].

We are able to improve the minimum visibility, however, by considering inequalities where B_Q is even closer to B_S than to B_L . In particular, we consider the “chained” or “Barrett-Kent-Pironio (BKP)” family of Bell inequalities [83,84], which generalize CHSH to the case of more settings. For our purposes, we express the BKP game between parties i and j as

$$S_k^{ij} = \sum_{l=1}^k \left[\langle A_l^i A_l^j \rangle + \langle A_{l+1}^i A_l^j \rangle \right] \leq 2k - 2, \quad (8)$$

where $A_{k+1}^i = -A_1^i$ and $\langle A_l^i A_l^j \rangle$ is the expectation value when the corresponding observables $A_l^i = \sum_{a_i} a_i M_{x_i=l}^{a_i}$ are measured by the distant parties. The BKP family of nonlocal games have the properties of

$$B_L = 2k - 2, \quad B_S = 2k, \quad B_Q = 2k \cos\left(\frac{\pi}{2k}\right), \quad B_N = 0, \quad (9)$$

where k denotes the number of settings available to each party. The BKP games are noteworthy for having $B_Q \rightarrow B_S$ as $k \rightarrow \infty$ [84] and for recovering the CHSH game when $k=2$. Does that mean that using more settings always improves the critical visibility for achieving SGMNL with parallel BKP games? No. In the limit $k \rightarrow \infty$, we also have B_L/B_Q approaching 1. Thus, every graph requires its own optimization. For the tripartite-line graph, we can witness SGMNL with $v > 0.947$ at $k=5$. For the triangle, however, the optimum number of settings is $k=3$, which witnesses SGMNL whenever $v > 0.899$.

Is it always the case that playing bipartite games in parallel per the triangle graph [Fig. 3(b)] collectively requires less visibility to witness SGMNL than playing bipartite games in parallel per the tripartite-line graph [Fig. 3(a)]? Yes, as we discuss next.

B. Optimization of the graph

Why does the triangle graph outperform the line graph? The answer is that in the triangle graph, no node has a vertex degree less than average. The total number of edges is equal to the number of nodes times the

average vertex degree divided by 2. By inspection of Corollary 3, it is clear that optimal graphs will have each node connected to the same number of edges. The technical term for such graphs is that they are *regular*. The triangle graph is regular; the tripartite-line graph is not. Let us take a moment to compute a visibility such that a regular graph will witness SGMNL per Corollary 3. If [number of edges connected to v] = d for all v , such that [number of edges of G] = $d/2 \times$ [number of nodes of G], then we have

$$v > \frac{1}{B_Q} \left(B_S - \frac{2 \times (B_S - B_L)}{\text{[number of nodes of } G]} \right). \quad (10)$$

This has two important consequences. First, the optimal network to witness SGMNL for parallel quantum nonlocal games is the triangle. Going to four or more parties only increases the requisite visibility. Second, achieving Svetlichnyesque *fully multipartite* nonlocal correlation for *any number of parties* N can evidently be realized by parallel playing suitably optimized BPK games in a regular graph with N nodes. Indeed, if we fix $k=N$, we find that $v > (N^2 - 2)/(N^2 \cos(\pi/2N))$, which is strictly less than 1 for all integer-valued $N \geq 3$.

We proceed, therefore, to implement parallel BPK games in the quantum triangle scenario with multiple settings per party.

IV. EXPERIMENTAL GENUINE TRIPARTITE NONLOCALITY IN THE TRIANGLE NETWORK

To experimentally implement the triangle network, we exploit the photonic platform of Fig. 4 with three different and separated polarization-entangled photon sources (ρ_{12} , ρ_{23} , and ρ_{13}). The source ρ_{12} generates photons by pumping a beta-barium-borate (BBO) crystal in pulsed mode, while the others, ρ_{13} and ρ_{23} , are composed of periodically poled potassium titanyl phosphate (PPKTP) crystals pumped by a continuous-wave laser. All three photon pairs exploit type-II degenerate spontaneous parametric down-conversion (SPDC) process. All the generated photons are distributed among the laboratories, i.e., one remains in the laboratory where it was generated while the other one is sent to the adjoining laboratory through optical fibers, the maximum length of which is 25 m. The three measurement stations, A_1 , A_2 , and A_3 , belonging to laboratories 1, 2, and 3, respectively, are composed by half-wave plates (HWP), quarter-wave plates (QWP), and polarizing beam splitters (PBS). At both outputs of each PBS, photons are coupled into single-mode fibers (SMFs) and directed to single-photon detectors (SPDs). The electronic signals generated by the detectors are sent to three time-to-digital converters (TDCs), each located at its respective measurement station.

The independence of the generated states is ensured by the location of the sources and the distinct lasers used as

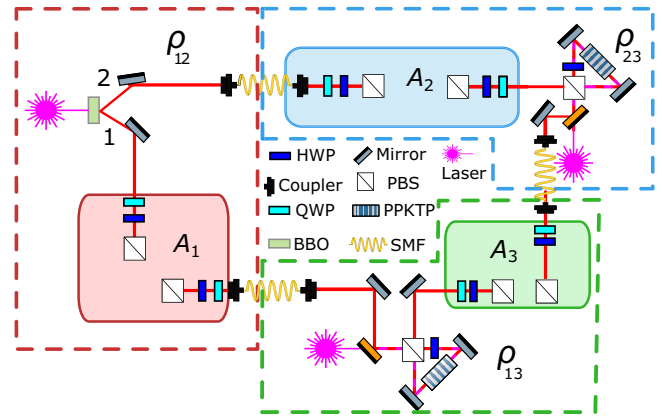


FIG. 4. The experimental apparatus. Three independent sources, ρ_{12} , ρ_{13} , and ρ_{23} , generate polarization-entangled photon pairs. A pump laser for source ρ_{12} with wavelength $\lambda = 397.5$ nm is produced by a second-harmonic-generation (SHG) process from a Ti:sapphire mode-locked laser with a repetition rate of 76 MHz and is focused on a 2-mm-thick beta-barium-borate (BBO) crystal. Sources ρ_{13} and ρ_{23} employ a continuous-wave diode laser, one for each source, with wavelength $\lambda = 404$ nm, which pumps a 20-mm-thick periodically poled potassium titanyl phosphate (PPKTP) crystal inside a Sagnac interferometer [85,86]. The photons generated in all the sources are filtered in wavelength and spatial mode by using narrow-band interference filters and single-mode fibers, respectively. Then, the photons are shared pairwise among three measurement stations, A_1 , A_2 , and A_3 , performing separable measurements on the pairs of incoming photons. Each measurement is performed in the polarization space of the photons, through a quarter-wave plate (QWP), a half-wave plate (HWP), and a polarizing beam splitter (PBS). In order to share photons along the stations in the triangle configuration, the photons are transmitted along single-mode fibers (SMFs) with lengths up to 25 m.

pumps. In particular, the quantum source generating ρ_{12} is supplied by a Ti:sapphire mode-locked laser, with a repetition rate of 76 MHz and wavelength of 397.5 nm. This impulsive pump laser is focused on 2-mm-thick BBO crystal. Instead, the quantum sources generating ρ_{23} and ρ_{13} are implemented by exploiting two independent continuous-wave diode lasers characterized by a wavelength of 404 nm and focused on distinct PPKTP crystals inside Sagnac interferometers. By pumping the crystal in the clockwise and anticlockwise paths of the interferometer, both of the signals can generate photon pairs through a collinear type-II SPDC process. Finally, recombining the two generations in the dual-wavelength PBS, the entangled photon pairs are obtained.

The three sources generate bipartite states, each of the form

$$\rho_{\text{exp}} = v |\Psi^-\rangle \langle \Psi^-| + (1-v) \times \left(\frac{\lambda}{2} (|\Psi^+\rangle \langle \Psi^+| + |\Psi^-\rangle \langle \Psi^-|) + \frac{1-\lambda}{4} \mathbb{I} \right), \quad (11)$$

where $|\Psi^\pm\rangle = (|10\rangle \pm |01\rangle)/\sqrt{2}$. They are a mixture of the maximally entangled state with colored and white noise, whose reconstructed densities matrices are reported in Supplemental Material [87].

To gauge the quality of the bipartite states, we optimize the violation of the CHSH inequality [88], corresponding to the chained inequality in Eq. (8), with $k = 2$ and being explicitly given by

$$S_2^{ij} = \langle A_1^i A_1^j \rangle + \langle A_2^i A_1^j \rangle + \langle A_2^i A_2^j \rangle - \langle A_1^i A_2^j \rangle \leq 2. \quad (12)$$

With our setup, we achieve the quantum violations of the classical bound given by $S_2^{12} = 2.643 \pm 0.002$, $S_2^{23} = 2.601 \pm 0.002$ and $S_2^{13} = 2.592 \pm 0.002$, values that unfortunately are not enough to violate the triangle SGMNL witness given in Eq. (5). These values are limited by the duration of the measurements combined with the stability of the whole experimental setup involving fiber connections with lengths up to 25 m distributing photons among the laboratories. However, as we show next, increasing the number of measurements (increasing k) is enough to counteract the unavoidable effects of noise and experimental errors and violate the SGMNL witness given in Eq. (5).

Experimentally, we test the triangle Svetlichny inequality in Eq. (5) on the BKP games in Eq. (8) with $k = 2, 3, 4$, and 5, obtaining a violation only for $k \geq 3$. Hereafter, we take $S_k^N := \sum_{i=1}^N S_k^{i,i\oplus 1}$, where \oplus denotes addition modulo N . More specifically, we obtain $S_2^{3,\text{exp}} = 7.835 \pm 0.003$, $S_3^{3,\text{exp}} = 14.632 \pm 0.006$, $S_4^{3,\text{exp}} = 20.388 \pm 0.004$ and $S_5^{3,\text{exp}} = 26.252 \pm 0.006$. For $k \geq 3$, the bounds in Eq. (5) are violated by 105, 97, and 45 standard deviations, respectively, for $k = 3, 4$, and 5. These results are summarized in Table I. The results are also presented in Fig. 5, where we show the ratio $S_k^{3,\text{exp}}/(6k - 4)$ [where $6k - 4$ is the classical bound of Eq. (5) applied to Eq. (8)]. As expected from the theoretical analysis, the larger ratio is obtained for $k = 3$.

The data acquisition is performed using three separated TDCs, with a time resolution of approximately 81

TABLE I. Considering the settings $k = 2, 3, 4$, and 5, the second column shows the classical bound $2B_L + B_s = 6k - 4$, the third column the quantum bound $3B_Q = 6k \cos(\frac{\pi}{2k})$, i.e., the maximum violation achievable with quantum correlations, and the fourth column shows the experimental violation achieved (a negative value implies no quantum violation).

Settings	Classical bound	Quantum bound	Experimental violation
k	$2B_L + B_s$	$3B_Q$	$S_k^{3,\text{exp}} - (6k - 4)$
2	8	8.48	-0.165 ± 0.003
3	14	15.59	0.632 ± 0.006
4	20	22.17	0.388 ± 0.004
5	26	28.53	0.252 ± 0.006

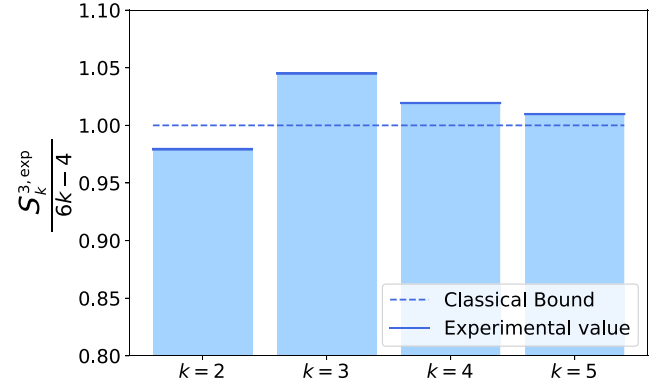


FIG. 5. Experimental results showing genuine tripartite nonlocality in the triangle network with inputs. The bars show the ratio $S_k^{3,\text{exp}}/(6k - 4)$ with numbers of settings $k = 2, 3, 4$, and 5 (note that the inequality is not violated for $k = 2$). The cyan bar charts represent the experimental data, while the dashed lines represent the classical bounds for the nonlocal Svetlichny model given in Eq. (3). The error bars are calculated taking into account the Poissonian errors relative to the measured counts and are depicted by the blue upper parts of the bars.

ps, recording the time stamps of all measured events at each station. In particular, each node is provided by a TDC synchronized with each other using a shared random signal, acting as a time reference. The time of the three nodes is sent to a separated machine that supplies real-time synchronization via dedicated software.

Subsequently, we employ two coincidence windows, w_1 and w_2 , for the collection of the sixfold events. The first window, w_1 , is needed to filter the pairs of photons, generated by the same source and so belonging to the same entangled pair. We use a value for it equal to approximately 3.24 ns, representing a good choice to filter out most of the noise due to accidental counts. The twofold coincidence rates computed distributing photons toward the different laboratories via optical fibers are approximately 2.5 kHz, 5.5 kHz, and 23 kHz, respectively, for ρ_{12} , ρ_{23} , and ρ_{31} . Conversely, the second window, w_2 , establishes when entangled pairs, generated by different sources, can be considered simultaneous as a sixfold event. By narrowing w_2 , the number of twofold coincidence events that are considered is reduced. This implies a larger uncertainty on the value of the quantum violations and it determines its fluctuations. We perform all measurements with different sixfold coincidence windows, i.e., the time interval where detection events are considered simultaneous, ranging from 0.405 to 63 μs . Within this range, the optimal value is chosen as a trade-off between two requirements. On the one hand, the entangled pairs generated by the two sources should be as close as possible in time, to approximate their simultaneity, even if there is no spacelike separation among the parties. On the other, an excessively narrow window implies that fewer coincidence events are retained

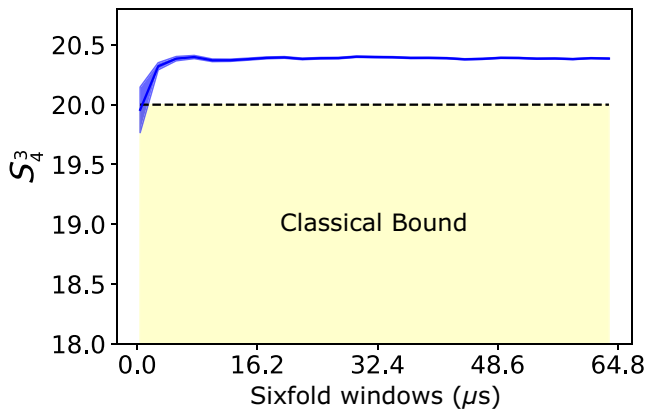


FIG. 6. The violation of S_4^3 as a function of the sixfold coincidence-window length. The blue line interpolates the experimental values of S_4^3 and the lighter blue region represents the relative Poissonian error.

in the analysis, which enlarges the relative uncertainty on the experimental frequencies and the corresponding quantum violations. Therefore, in our analysis, we choose the value $w_2 = 61 \mu\text{s}$. Using such a window, we reach a sixfold coincidence rate equal to approximately 300 Hz. As an illustration of the role of these time windows, in Fig. 6 we report the obtained violation of the SGMNL witness given in Eq. (5) as a function of this window, showing as its uncertainty, represented by the blue area, decreases by increasing the window. Moreover, by enlarging the sixfold window, the scheme is able to generate multiphoton states from different kinds of nonsynchronized sources.

V. DISCUSSION AND CONCLUSIONS

Historically, the primary interest in quantum networks has been the study of communication networks relevant to modeling the different scales of quantum Internet [12, 54,55]. More recently, however, quantum networks have emerged to take a central place in the foundations of quantum theory. This stems from an appreciation of that Bell’s theorem—the focus of the community for a long period of time—represents only a particular such network at the interface between quantum information and causality theory [24,25,27–32,34–52]. The imposition of different causal structures in quantum experiments allows us to probe the insufficiency of classical explanations in new regimes and thus to identify new—and in some cases *stronger*—forms of nonclassical behavior.

Within this context, our main goal is to demonstrate the possibility of achieving genuine multipartite nonlocality by having the parties merely perform local measurements on bipartite entanglement sources distributed in a network. Our theoretical analysis in Sec. III identifies the tripartite-triangle-graph nonlocal game as the *most* suitable configuration of parallel-bipartite nonlocal games to

robustly realize genuine multipartite nonlocality. The corresponding causal structure—which forms the basis for our experimental implementation—is the so-called triangle network, a causal scenario that has been at the focus of extensive theoretical analysis recently [25,27–39]. Whereas most prior literature has considered a form of triangle network without inputs to the measurements of the parties and without shared randomness, here we consider more traditional multipartite nonlocal games. The salient common feature, however, is the independence of the three sources of quantum states.

As expected, our experimental results are inconsistent with any LHV model; that is, we achieve nonlocal correlations. It is much more significant, however, that our experimental results are, furthermore, inconsistent with a *stronger* classical causal hypothesis, namely, Svetlichny’s classical foil theory, which allows for any two of the three parties to communicate their inputs to coordinate their outputs with each other [67].

Thus, employing our photonic setup, we experimentally realize genuine tripartite nonlocality. Our operational witness of this fact is the violation of a class of Bell inequalities rederived in Lemma 1. Such inequalities have initially been considered in Ref. [50]; they consist of the parallel testing of the chained (i.e., BKP) Bell inequalities [83,84] between multiple pairs of distinct parties. Violation of such a combined multipartite inequality unambiguously witnesses Svetlichnyesque genuine multipartite nonlocality.

To be clear, we are not claiming to be the first experiment to violate inequalities bounding the correlations consistent with Svetlichny’s classical foil theory. Reference [89], for example, certainly does so already. What distinguishes our demonstration from prior ones, however, is that prior experimental realizations of Svetlichnyesque genuine tripartite nonlocality have relied on a single tripartite system with high fidelity Greenberger-Horne-Zeilinger (GHZ) state. By contrast, our demonstration requires only *bipartite* sources of entangled states. Notably, bipartite states can be easily prepared with higher coincidence rate and fidelities with respect to the GHZ states [89–96] and thus offer a more scalable platform with the cost of relaxing the simultaneity of events.

Importantly, Svetlichny’s causal model has also found applications for the detection and quantification of multipartite entanglement [49,97,98] as well as in cryptographic applications such as secret sharing [99]. Notwithstanding this, all these applications have had in mind a single source of correlations rather than the network we consider here. We believe that exploring the protocols and applications opened up by the quantum triangle and its generalizations to growing networks is a promising venue for future research, an area in which we hope our results might provoke further developments.

ACKNOWLEDGMENTS

We thank Robert Spekkens for the fruitful discussions. This work was supported by The John Templeton Foundation via The Quantum Information Structure of Spacetime (QISS) Project [100] [the opinions expressed in this publication are those of the author(s) and do not necessarily reflect the views of the John Templeton Foundation] Grant Agreement No. 61466, by the Ministry of Education, University, and Research (MIUR) via Progetto di Ricerca di Interesse Nazionale (PRIN) 2017 project “‘Taming complexity with quantum strategies: A hybrid integrated photonics approach” (QUSHIP) (2017SRNBRK), by the Regione Lazio program “Progetti di Gruppi di ricerca” legge Regionale n. 13/2008 (‘trattamento Sicuro di dati mediante l’iNFORMazione con singoli fotoNI A richiesta’ (SINFONIA) project, Grant No. 85-2017-15200) via Lazio Innova S.p.A., and by the European Research Council (ERC) Advanced Grant “QUantum advantage via non-linear BOSon Sampling” (QU-BOSS) (Grant Agreement No. 884676). This work was also supported by the Serrapilheira Institute (Grant No. Serra—1708-15763). Research at Perimeter Institute is supported in part by the Government of Canada through the Department of Innovation, Science and Economic Development and by the Province of Ontario through the Ministry of Colleges and Universities. R.C. and A.C. also acknowledge the Brazilian National Council for Scientific and Technological Development (CNPq) via the National Institute for Science and Technology on Quantum Information (INCT-IQ) and Grants No. 406574/2018-9 and No. 307295/2020-6 and the Brazilian agencies Ministry of Technology, Innovations, and Communication (MCTIC) and Ministry of Education (MEC).

-
- [1] J. S. Bell, On the Einstein Podolsky Rosen Paradox, *Physics Physique Fizika* **1**, 195 (1964).
- [2] N. Brunner, D. Cavalcanti, S. Pironio, V. Scarani, and S. Wehner, Bell nonlocality, *Phys. Mod. Phys.* **86**, 419 (2014).
- [3] V. Scarani, *Bell Nonlocality* (Oxford University Press, 2019).
- [4] L. K. Shalm, E. Meyer-Scott, B. G. Christensen, P. Bierhorst, M. A. Wayne, M. J. Stevens, T. Gerrits, S. Glancy, D. R. Hamel, M. S. Allman, *et al.*, Strong Loophole-Free Test of Local Realism, *Phys. Rev. Lett.* **115**, 250402 (2015).
- [5] M. Giustina, M. A. M. Versteegh, S. Wengerowsky, J. Handsteiner, A. Hochrainer, K. Phelan, F. Steinlechner, J. Kofler, J.-Å. Larsson, C. Abellán, *et al.*, Significant-Loophole-Free Test of Bell’s Theorem with Entangled Photons, *Phys. Rev. Lett.* **115**, 250401 (2015).
- [6] B. Hensen, H. Bernien, A. E. Dréau, A. Reiserer, N. Kalb, M. S. Blok, J. Ruitenberg, R. F. Vermeulen, R. N. Schouten, C. Abellán, W. Amaya, V. Pruneri, M. W. Mitchell, M. Markham, D. J. Twitchen, D. Elkouss, S. Wehner, T. H. Tamini, and R. Hanson, Loophole-free Bell inequality violation using electron spins separated by 1.3 kilometres, *Nature* **526**, 682 (2015).
- [7] B. B. T. Collaboration *et al.*, Challenging local realism with human choices, *Nature* **557**, 212 (2018).
- [8] N. Gisin and R. Thew, Quantum communication, *Nat. Photonics* **1**, 165 (2007).
- [9] V. Scarani, H. Bechmann-Pasquinucci, N. J. Cerf, M. Dušek, N. Lütkenhaus, and M. Peev, The security of practical quantum key distribution, *Phys. Mod. Phys.* **81**, 1301 (2009).
- [10] S. Pironio, L. Masanes, A. Leverrier, and A. Acín, Security of Device-Independent Quantum Key Distribution in the Bounded-Quantum-Storage Model, *Phys. Rev. X* **3**, 031007 (2013).
- [11] F. B. Basset, M. Valeri, E. Roccia, V. Muredda, D. Poderini, J. Neuwirth, N. Spagnolo, M. B. Rota, G. Carvacho, *et al.*, Quantum key distribution with entangled photons generated on demand by a quantum dot, *Sci. Adv.* **7**, eabe6379 (2021).
- [12] Y.-A. Chen, Q. Zhan, T.-Y. Chen, W.-Q. Cai, S.-K. Liao, J. Zhang, K. Chen, J. Yin, J.-G. Ren, Z. Chen, *et al.*, An integrated space-to-ground quantum communication network over 4,600 kilometres, *Nature* **589**, 214 (2021).
- [13] Y.-B. Sheng, L. Zhou, and G.-L. Long, One-step quantum secure direct communication, *Sci. Bull.* **67**, 367 (2022).
- [14] S. Pironio, A. Acín, S. Massar, A. B. de La Giroday, D. N. Matsukevich, P. Maunz, S. Olmschenk, D. Hayes, L. Luo, *et al.*, Random numbers certified by Bell’s theorem, *Nature* **464**, 1021 (2010).
- [15] A. Acín and L. Masanes, Certified randomness in quantum physics, *Nature* **540**, 213 (2016).
- [16] M. N. Bera, A. Acín, M. Kuś, M. W. Mitchell, and M. Lewenstein, Randomness in quantum mechanics: Philosophy, physics and technology, *Rep. Prog. Phys.* **80**, 124001 (2017).
- [17] I. Agresti, D. Poderini, L. Guerini, M. Mancusi, G. Carvacho, L. Aolita, D. Cavalcanti, R. Chaves, and F. Sciarrino, Experimental device-independent certified randomness generation with an instrumental causal structure, *Commun. Phys.* **3**, 1 (2020).
- [18] D. Poderini, E. Polino, G. Rodari, A. Suprano, R. Chaves, and F. Sciarrino, Ab initio experimental violation of Bell inequalities, *Phys. Rev. Res.* **4**, 013159 (2022).
- [19] I. Šupić and J. Bowles, Self-testing of quantum systems: a review, *Quantum* **4**, 337 (2020).
- [20] H. Buhman, R. Cleve, S. Massar, and R. De Wolf, Non-locality and communication complexity, *Rev. Mod. Phys.* **82**, 665 (2010).
- [21] J. Ho, G. Moreno, S. Brito, F. Graffitti, C. L. Morrison, R. Nery, A. Pickston, M. Proietti, R. Rabelo, and A. Fedrizzi *et al.*, [arXiv:2106.06552](https://arxiv.org/abs/2106.06552) (2021).
- [22] C. J. Wood and R. W. Spekkens, The lesson of causal discovery algorithms for quantum correlations: Causal explanations of Bell-inequality violations require fine-tuning, *New J. Phys.* **17**, 033002 (2015).
- [23] R. Chaves, R. Kueng, J. B. Brask, and D. Gross, Unifying Framework for Relaxations of the Causal Assumptions in Bell’s Theorem, *Phys. Rev. Lett.* **114**, 140403 (2015).

- [24] T. Fritz, Beyond Bell's theorem: Correlation scenarios, *New J. Phys.* **14**, 103001 (2012).
- [25] M.-O. Renou, E. Bäumer, S. Boreiri, N. Brunner, N. Gisin, and S. Beigi, Genuine Quantum Nonlocality in the Triangle Network, *Phys. Rev. Lett.* **123**, 140401 (2019).
- [26] N. Gisin, [arXiv:1708.05556](https://arxiv.org/abs/1708.05556) (2017).
- [27] N. Gisin, Entanglement 25 years after quantum teleportation: Testing joint measurements in quantum networks, *Entropy* **21**, 325 (2019).
- [28] T. Kriváchy, Y. Cai, D. Cavalcanti, A. Tavakoli, N. Gisin, and N. Brunner, A neural network oracle for quantum nonlocality problems in networks, *npj Quantum Inf.* **6**, 70 (2020).
- [29] E. Bäumer, N. Gisin, and A. Tavakoli, Demonstrating the power of quantum computers, certification of highly entangled measurements and scalable quantum nonlocality, *npj Quantum Inf.* **7**, 1 (2021).
- [30] J. Henson, R. Lal, and M. F. Pusey, Theory-independent limits on correlations from generalized Bayesian networks, *New J. Phys.* **16**, 113043 (2014).
- [31] R. Chaves, C. Majenz, and D. Gross, Information-theoretic implications of quantum causal structures, *Nat. Commun.* **6**, 1 (2015).
- [32] B. Steudel and N. Ay, Information-theoretic inference of common ancestors, *Entropy* **17**, 2304 (2015).
- [33] T. Fritz, Beyond Bell's theorem II: Scenarios with arbitrary causal structure, *Comm. Math. Phys.* **341**, 391 (2016).
- [34] T. C. Fraser and E. Wolfe, Causal compatibility inequalities admitting quantum violations in the triangle structure, *Phys. Rev. A* **98**, 022113 (2018).
- [35] E. Wolfe, R. W. Spekkens, and T. Fritz, The inflation technique for causal inference with latent variables, *J. Caus. Inf.* **7**, 20170020 (2019).
- [36] J. Åberg, R. Nery, C. Duarte, and R. Chaves, Semidefinite Tests for Quantum Network Topologies, *Phys. Rev. Lett.* **125**, 110505 (2020).
- [37] T. Kraft, S. Designolle, C. Ritz, N. Brunner, O. Gühne, and M. Huber, Quantum entanglement in the triangle network, *Phys. Rev. A* **103**, L060401 (2021).
- [38] I. Šupić, J.-D. Bancal, and N. Brunner, Quantum Nonlocality in Networks Can Be Demonstrated with an Arbitrarily Small Level of Independence between the Sources, *Phys. Rev. Lett.* **125**, 240403 (2020).
- [39] M.-O. Renou, Y. Wang, S. Boreiri, S. Beigi, N. Gisin, and N. Brunner, Limits on Correlations in Networks for Quantum and No-Signaling Resources, *Phys. Rev. Lett.* **123**, 070403 (2019).
- [40] C. Branciard, D. Rosset, N. Gisin, and S. Pironio, Bilocal versus nonbilocal correlations in entanglement-swapping experiments, *Phys. Rev. A* **85**, 032119 (2012).
- [41] R. Chaves, L. Luft, and D. Gross, Causal structures from entropic information: Geometry and novel scenarios, *New J. Phys.* **16**, 043001 (2014).
- [42] R. Chaves, Polynomial Bell Inequalities, *Phys. Rev. Lett.* **116**, 010402 (2016).
- [43] A. Tavakoli, N. Gisin, and C. Branciard, Bilocal Bell Inequalities Violated by the Quantum Elegant Joint Measurement, *Phys. Rev. Lett.* **126**, 220401 (2021).
- [44] A. Tavakoli, P. Skrzypczyk, D. Cavalcanti, and A. Acín, Nonlocal correlations in the star-network configuration, *Phys. Rev. A* **90**, 062109 (2014).
- [45] N. Gisin, Q. Mei, A. Tavakoli, M. O. Renou, and N. Brunner, All entangled pure quantum states violate the bilocality inequality, *Phys. Rev. A* **96**, 020304 (2017).
- [46] D. Poderini, R. Chaves, I. Agresti, G. Carvacho, and F. Sciarrino, in *Proc. 35th UAI Conf.* (PMLR, Tel Aviv, Israel, 2020), p. 1274.
- [47] A. Tavakoli, M. O. Renou, N. Gisin, and N. Brunner, Correlations in star networks: From Bell inequalities to network inequalities, *New J. Phys.* **19**, 073003 (2017).
- [48] D. Rosset, C. Branciard, T. J. Barnea, G. Pütz, N. Brunner, and N. Gisin, Nonlinear Bell Inequalities Tailored for Quantum Networks, *Phys. Rev. Lett.* **116**, 010403 (2016).
- [49] J.-D. Bancal, C. Branciard, N. Gisin, and S. Pironio, Quantifying Multipartite Nonlocality, *Phys. Rev. Lett.* **103**, 090503 (2009).
- [50] R. Chaves, D. Cavalcanti, and L. Aolita, Causal hierarchy of multipartite Bell nonlocality, *Quantum* **1**, 23 (2017).
- [51] N. Gisin, J.-D. Bancal, Y. Cai, P. Remy, A. Tavakoli, E. Zambrini Cruzeiro, S. Popescu, and N. Brunner, Constraints on nonlocality in networks from no-signaling and independence, *Nature Comm.* **11**, 2378 (2020).
- [52] A. Canabarro, S. Brito, and R. Chaves, Machine Learning Nonlocal Correlations, *Phys. Rev. Lett.* **122**, 200401 (2019).
- [53] R. Chaves, G. Moreno, E. Polino, D. Poderini, I. Agresti, A. Suprano, M. R. Barros, G. Carvacho, E. Wolfe, *et al.*, Causal Networks and Freedom of Choice in Bell's Theorem, *PRX Quantum* **2**, 040323 (2021).
- [54] S. Wehner, D. Elkouss, and R. Hanson, Quantum Internet: A vision for the road ahead, *Science* **362**, 6412 (2018).
- [55] S. Brito, A. Canabarro, R. Chaves, and D. Cavalcanti, Statistical Properties of the Quantum Internet, *Phys. Rev. Lett.* **124**, 210501 (2020).
- [56] A. Tavakoli, A. Pozas-Kerstjens, M. X. Luo, and M.-O. Renou, Bell nonlocality in networks, *Rep. Prog. Phys.* **85**, 056001 (2022).
- [57] G. Carvacho, F. Andreoli, L. Santodonato, M. Bentivegna, R. Chaves, and F. Sciarrino, Experimental violation of local causality in a quantum network, *Nat. Commun.* **8**, 1 (2017).
- [58] D. J. Saunders, A. J. Bennet, C. Branciard, and G. J. Pryde, Experimental demonstration of nonbilocal quantum correlations, *Sci. Adv.* **3**, e1602743 (2017).
- [59] F. Andreoli, G. Carvacho, L. Santodonato, M. Bentivegna, R. Chaves, and F. Sciarrino, Experimental bilocality violation without shared reference frames, *Phys. Rev. A* **95**, 062315 (2017).
- [60] R. Chaves, G. Carvacho, I. Agresti, V. Di Giulio, L. Aolita, S. Giacomini, and F. Sciarrino, Quantum violation of an instrumental test, *Nat. Phys.* **14**, 291 (2018).
- [61] E. Polino, I. Agresti, D. Poderini, G. Carvacho, G. Milani, G. B. Lemos, R. Chaves, and F. Sciarrino, Device-independent test of a delayed choice experiment, *Phys. Rev. A* **100**, 022111 (2019).

- [62] G. Carvacho, R. Chaves, and F. Sciarrino, Perspective on experimental quantum causality, *EPL (Europhysics Letters)* **125**, 30001 (2019).
- [63] Q.-C. Sun, Y.-F. Jiang, B. Bai, W. Zhang, H. Li, X. Jiang, J. Zhang, L. You, X. Chen, *et al.*, Experimental demonstration of non-bilocality with truly independent sources and strict locality constraints, *Nat. Photonics* **13**, 687 (2019).
- [64] D. Poderini, I. Agresti, G. Marchese, E. Polino, T. Giordani, A. Suprano, M. Valeri, G. Milani, N. Spagnolo, *et al.*, Experimental violation of n-locality in a star quantum network, *Nat. Commun.* **11**, 1 (2020).
- [65] G. Carvacho, E. Roccia, M. Valeri, F. B. Basset, D. Poderini, C. Pardo, E. Polino, L. Carosini, M. B. Rota, and J. Neuwirth *et al.*, *Optica* **9**, 572 (2022).
- [66] Note that these experiments have not simultaneously closed the locality and detection-efficiency loophole. Nonetheless, up to to these loopholes, in some of these experiments the violation of Bell inequalities relies solely on the experimental data, without the need of assumptions on the state-preparation-and-measurement devices.
- [67] G. Svetlichny, Distinguishing three-body from two-body nonseparability by a Bell-type inequality, *Phys. Rev. D* **35**, 3066 (1987).
- [68] R. Gallego, L. E. Würflinger, A. Acín, and M. Navascués, Operational Framework for Nonlocality, *Phys. Rev. Lett.* **109**, 070401 (2012).
- [69] J.-D. Bancal, J. Barrett, N. Gisin, and S. Pironio, Definitions of multipartite nonlocality, *Phys. Rev. A* **88**, 014102 (2013).
- [70] D. Cavalcanti, M. L. Almeida, V. Scarani, and A. Acín, Quantum networks reveal quantum nonlocality, *Nat. Commun.* **2**, 1 (2011).
- [71] M. L. Almeida, D. Cavalcanti, V. Scarani, and A. Acín, Multipartite fully nonlocal quantum states, *Phys. Rev. A* **81**, 052111 (2010).
- [72] P. Contreras-Tejada, C. Palazuelos, and J. I. de Vicente, Genuine Multipartite Nonlocality Is Intrinsic to Quantum Networks, *Phys. Rev. Lett.* **126**, 040501 (2021).
- [73] S. Pironio, PhD thesis, Universit Libre de Bruxelles, 2004.
- [74] J. Barrett, N. Linden, S. Massar, S. Pironio, S. Popescu, and D. Roberts, Nonlocal correlations as an information-theoretic resource, *Phys. Rev. A* **71**, 022101 (2005).
- [75] J. Pearl, *Causality*, 2nd ed. (Cambridge University Press, Cambridge, 2009).
- [76] J.-M. A. Allen, J. Barrett, D. C. Horsman, C. M. Lee, and R. W. Spekkens, Quantum Common Causes and Quantum Causal Models, *Phys. Rev. X* **7**, 031021 (2017).
- [77] J. Barrett and S. Pironio, Popescu-Rohrlich Correlations as a Unit of Nonlocality, *Phys. Rev. Lett.* **95**, 140401 (2005).
- [78] We can treat the physical devices in a Bell experiment as boxes, each distant part having local access to part of it, via the inputs it chooses and the corresponding outcomes that it obtains. Local wirings correspond then to transformations that we can perform in such boxes. For instance, if two parties share two copies of a box, they can use the outputs of one box as the input of the other.
- [79] Lemma 1 holds for *all* GMNL variant definitions as introduced in Refs. [68,69], since signaling boxes provide no advantage over generic nonsignaling boxes when evaluating any subset instance of a nonlocal game.
- [80] B. S. Cirel'son, Quantum generalizations of Bell's inequality, *Lett. Mat. Phys.* **4**, 93 (1980).
- [81] Note that this explicit construction holds for all GMNL variants defined in Refs. [68,69].
- [82] X. Coiteux-Roy, E. Wolfe, and M.-O. Renou, No Bipartite-Nonlocal Causal Theory Can Explain Nature's Correlations, *Phys. Rev. Lett.* **127**, 200401 (2021).
- [83] S. L. Braunstein and C. M. Caves, Wringing out better Bell inequalities, *Ann. Phys.* **202**, 22 (1990).
- [84] J. Barrett, A. Kent, and S. Pironio, Maximally Nonlocal and Monogamous Quantum Correlations, *Phys. Rev. Lett.* **97**, 170409 (2006).
- [85] T. Kim, M. Fiorentino, and F. N. Wong, Phase-stable source of polarization-entangled photons using a polarization Sagnac interferometer, *Phys. Rev. A* **73**, 012316 (2006).
- [86] A. Fedrizzi, T. Herbst, A. Poppe, T. Jennewein, and A. Zeilinger, A wavelength-tunable fiber-coupled source of narrowband entangled photons, *Opt. Express* **15**, 15377 (2007).
- [87] See Supplemental Material at <http://link.aps.org/supplemental/10.1103/PRXQuantum.3.030342> for details about the experimental density matrices reconstructed through quantum state tomography.
- [88] J. F. Clauser, M. A. Horne, A. Shimony, and R. A. Holt, Proposed Experiment to Test Local Hidden Variable Theories, *Phys. Rev. Lett.* **23**, 880 (1969).
- [89] J. Lavoie, R. Kaltenbaek, and K. J. Resch, Experimental violation of Svetlichny's inequality, *New J. Phys.* **11**, 073051 (2009).
- [90] D. R. Hamel, L. K. Shalm, H. Hübel, A. J. Miller, F. Marsili, V. B. Verma, R. P. Mirin, S. W. Nam, K. J. Resch, and T. Jennewein, Direct generation of three-photon polarization entanglement, *Nat. Photonics* **8**, 801 (2014).
- [91] Z. M. Chaisson, P. F. Poitras, M. Richard, Y. Castonguay-Pagé, P.-H. Glinel, V. Landry, and D. R. Hamel, Phase-stable source of high-quality three-photon polarization entanglement by cascaded down-conversion, *Phys. Rev. A* **105**, 063705 (2022).
- [92] X.-L. Wang, L.-K. Chen, W. Li, H.-L. Huang, C. Liu, C. Chen, Y.-H. Luo, Z.-E. Su, D. Wu, Z.-D. Li, H. Lu, Y. Hu, X. Jiang, C.-Z. Peng, L. Li, N.-L. Liu, Y.-A. Chen, C.-Y. Lu, and J.-W. Pan, Experimental Ten-Photon Entanglement, *Phys. Rev. Lett.* **117**, 210502 (2016).
- [93] D. Bouwmeester, J.-W. Pan, M. Daniell, H. Weinfurter, and A. Zeilinger, Observation of Three-Photon Greenberger-Horne-Zeilinger Entanglement, *Phys. Rev. Lett.* **82**, 1345 (1999).
- [94] J.-W. Pan, D. Bouwmeester, M. Daniell, H. Weinfurter, and A. Zeilinger, Experimental test of quantum nonlocality in three-photon Greenberger-Horne-Zeilinger entanglement, *Nature* **403**, 515 (2000).
- [95] L. Huang, X.-M. Gu, Y.-F. Jiang, D. Wu, B. Bai, M.-C. Chen, Q.-C. Sun, J. Zhang, S. Yu, and Q. Zhang *et al.*, Experimental Demonstration of Genuine Tripartite Nonlocality under Strict Locality Conditions, *Phys. Rev. Lett.* **129**, 060401 (2022).

- [96] H. Cao, M.-O. Renou, C. Zhang, G. Massé, X. Coiteux-Roy, B.-H. Liu, Y.-F. Huang, C.-F. Li, G.-C. Guo, and E. Wolfe, Experimental demonstration that no tripartite-nonlocal causal theory explains Nature's correlations (2022).
- [97] T. Moroder, J.-D. Bancal, Y.-C. Liang, M. Hofmann, and O. Gühne, Device-Independent Entanglement Quantification and Related Applications, *Phys. Rev. Lett.* **111**, 030501 (2013).
- [98] J. T. Barreiro, J.-D. Bancal, P. Schindler, D. Nigg, M. Hennrich, T. Monz, N. Gisin, and R. Blatt, Demonstration of genuine multipartite entanglement with device-independent witnesses, *Nat. Phys.* **9**, 559 (2013).
- [99] M. Moreno, S. Brito, R. V. Nery, and R. Chaves, Device-independent secret sharing and a stronger form of Bell nonlocality, *Phys. Rev. A* **101**, 052339 (2020).
- [100] The Quantum Information Structure of Spacetime (QISS) Project, <https://www.qiss.fr>.